Dynamic fracture behavior of high-strength concrete studied by means of a drop-weight impact machine

X.X. Zhang[1,2], G. Ruiz[1], R.C. Yu[1], M. Tarifa[1]
[1] *Universidad de Castilla-La Mancha, Ciudad Real, Spain;* [2] *Harbin Engineering University, Harbin, China;*

Abstract: Three-point bending tests on notched beams of a high-strength concrete have been conducted using both a servo-hydraulic machine and a self-designed drop-weight impact device. The work of fracture and the peak load were measured over a wide range of displacement rates (loading rates). Under low displacement rates, from 10^{-4} mm/s to 10 mm/s, the tests were performed with the servo-hydraulic machine; from 10^{2} mm/s to 10^{3} mm/s we used the drop-weight impact machine instead. The results show that the work of fracture and the peak load increase as the displacement velocity increases. Nevertheless, such trend is relatively mild under low rates and can be attributed to viscous effects mainly originated by the presence of water in the pore structure. Under high rates the increases in the work of fracture and in the peak load are dramatic due to the effect of inertia.

1. Introduction

Nowadays high strength concrete (HSC) is very often used in modern complicated structures of considerable height and span, such as skyscrapers, high towers and large bridges. These are more vulnerable to damages caused by earthquakes, wind and blast loading owing to the fact that HSC is more brittle than normal strength concrete (NSC). Hence the dynamic fracture properties of HSC are more important than those of NSC with regard to safety assessment and the design of modern structures.

Over the past few decades, compared with the extensive research into the static fracture behavior of HSC [1-16], much less information is available on its dynamic fracture behavior.

Thus, in order to get additional insights into the loading rate effect on the fracture properties of HSC, in this paper we present three-point bending tests conducted at wide loading rates, from 10^{-4} mm/s to 10^{3} mm/s, using both a hydraulic servo-controlled testing machine and a drop-weight impact instrument. The results show that both the work of fracture and the peak load increase with the increase in loading rates. Under low loading rates, such tendency is mild, while it is remarkable instead under high loading rates. This paper also provides formulations for the rate-dependency of the work of fracture and of the peak load, the model will be helpful when simulating such rate dependency numerically.

The paper is structured as follows: the experimental procedure is given in section 2, in section 3 the results are presented and discussed. Section 4 shows the comparison with data in the literature. Finally, some conclusions are drawn in section 5.

2. Experimental procedure

2.1 Material characterization

A single high strength concrete was used throughout the experiments, made with a Porphyry aggregate of 12 mm maximum size and ASTM type I cement, I52.5R. Microsilica fume slurry and super plasticizer (Glenium ACE 325, B225) were used in the concrete composition. The water to cement ratio, *w/c* was fixed at 0.25%.

There was a strict control of the specimen-making process, to minimize scattering in test results. All of the specimens were cast in steel molds, vibrated by a vibrating table, wrap-cured for 24 hours, demolded, and stored for 4 weeks in a moist chamber at 20℃ and 98% relative humidity until they were tested.

Compressive tests were conducted according to ASTM C39 and C469 on 75 mm×150 mm (diameter × height) cylinders. Brazilian tests were also carried out using the same dimensional cylinders following the procedures recommended by ASTM C496. We made 8 cylinders, 4 for compression tests and 4 for splitting tests. Table 1 shows the characteristic mechanical parameters of the concrete determined in the various characterization and control tests. The mass density of the material is 2400 kg/m^3.

Table 1 Mechanical properties of the high-strength concrete

	f_c (MPa)	f_t (MPa)	E_c (GPa)
1	115.6	6.8	44.5
2	133.7	5.7	44.9
3	119.7	5.9	40.4
4	138.9	6.8	43.3
Mean	127.0	6.3	43.3
Std. Dev	11.1	0.6	2.0

2.2 Three-point bending fracture tests

To study the loading rate effect on the fracture behaviour of the HSC, three-point bending tests on notched beams were conducted in a wide loading rate range, from 10^{-4} mm/s to 10^3 mm/s. Two testing machines were adopted to carry out tests, one is a hydraulic servo-controlled testing machine, and the other is a self-designed drop-weight impact instrument.

The dimensions of the test beams were 100×100 mm^2 (B×D) in cross section, and 400 mm (L) in total length. The initial notch-depth ratio (a/D) was approximately 0.5, and the span (S) was fixed at 300 mm during the tests.

2.2.1 Tests under loading rates from 10^{-4} mm/s to 10^{1} mm/s

In this low loading rate range, the tests were performed using the hydraulic serve-controlled testing machine.

In regard to the measuring method for the work of fracture (W_F), we followed the procedures devised by Elices, Guinea and Planas [17-20]. The tests were performed in position-control. Three loading rates were applied during the test from quasi-static level (5.50×10^{-4} mm/s) to rate dependent levels (5.50×10^{-1} mm/s and 1.74×10^{1} mm/s). Three specimens were tested at each loading rate.

2.2.2 Tests under loading rates from 10^{2} mm/s to 10^{3} mm/s

In this high loading rates range, all impact tests were conducted using the instrumented, drop-weight impact apparatus designed and constructed in the Laboratory of Materials and Structures of Universidad de Castilla – La Mancha. It has the capacity of dropping 316 kg mass from heights of up to 2.6 m, and can accommodate flexural specimens with spans up to about 1.6 m. In this study, an impact hammer weighing 120.6 kg was used, three drop heights were adopted, 40, 160 and 360 mm, respectively.

A detailed description of the instrument is given in reference [21]. The impact force between the hammer tup and the specimen is measured by a piezoelectric force sensor. Moreover, the reaction force between the support and the specimen is determined by another two force sensors.

An accelerometer bonded on the impact hammer was used to measure acceleration and displacement during the impact process. By assuming that the hammer displacement was essentially equal to the specimen deformation, the velocity and the loading point displacement could be evaluated using the equations as follows [22].

The initial impact velocity of the hammer, $\dot{u}_h(0)$ is

$$\dot{u}_h(0) = \sqrt{2aH} \tag{1}$$

where a is the corrected gravitational acceleration ($9.71 \pm 0.14 m/s^2$), H stands for the hammer drop height. During the impact process, the velocity of the hammer can be obtained using Eq. 2.

$$\dot{u}_h(t) = \dot{u}_h(0) + \int_0^t \ddot{u}_h(t)dt \tag{2}$$

where $\ddot{u}_h(t)$ is the recorded acceleration by the accelerometer bonded on the hammer. Then, the displacement of the hammer, $u_h(t)$ and also the loading point displacement of the specimen is calculated by Eq. 3.

$$u_h(t) = \int_0^t \left[\dot{u}_h(0) + \int_0^t \ddot{u}_h(t)dt \right] dt \tag{3}$$

Regarding the measuring method for the work of fracture, it is calculated by the area under the reaction force-displacement (load-displacement) curves, where the reaction force is evaluated by summing the values from both support data points[21,23].

3. Results and discussion

Fig. 1 shows the comparison of the typical load-displacement curves at different loading rates. It is obvious that the peak load increases with the increase in loading rates. On the contrary, the stiffness of the beam does not show similar tendency, which is due to the sensitivity of the elastic flexibility of the beam to the boundary conditions during the application of the concentrated load [24].

Table 2 shows detailed information on the experimental results. The data in the parenthesis are the standard deviation, dynamic increase factor (*DIF*), is defined by the ratio of peak load (P_{max}) and work of fracture to the corresponding quasi-static one, respectively. Here, the lowest loading rate ($\dot{\delta} = 5.50 \times 10^{-4}$ mm/s) is taken as the quasi-static loading condition. *H* stands for the dropping height of the hammer under impact loading conditions.

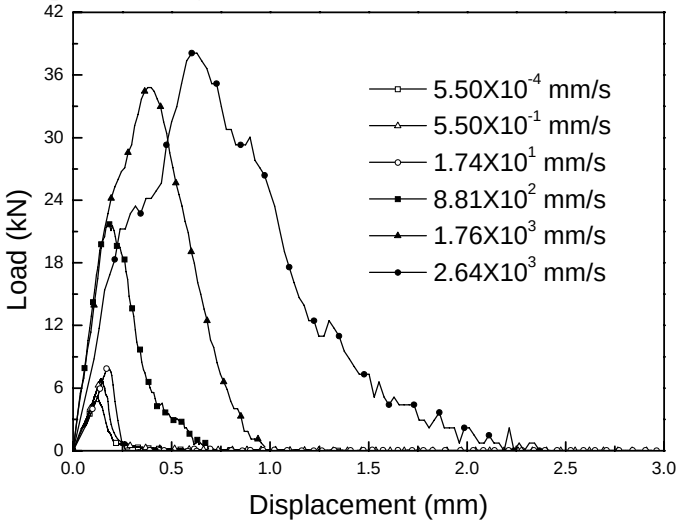

Fig. 1. Load-displacement curves at different loading rates.

Table 2 Experimental results at different loading rates

Testing machine	H (mm)	$\dot{\delta}$ (mm/s)	P_{max} (kN)	DIF for P_{max}	W_F (N/m)	DIF for W_F
Hydraulic serve-controlled device	-	5.50×10^{-4}	5.33 (0.33)	1	148 (9)	1
	-	5.50×10^{-1}	7.20 (0.30)	1.35	205 (12)	1.38
	-	1.74×10^{1}	8.22 (0.37)	1.54	226 (19)	1.52
Drop-weight impact instrument	40	8.81×10^{2}	23.87 (3.10)	4.48	1205 (24)	8.12
	160	1.76×10^{3}	34.34 (2.73)	6.44	3968 (653)	26.74
	360	2.64×10^{3}	38.07 (7.65)	7.14	5658 (885)	38.12

Fig. 2 shows the loading rate effect on the work of fracture. It is clear that the work of fracture increases with the increase in loading rates, while beyond a threshold (7.04×10^{2} mm/s) the rate effect becomes more pronounced and a significant increase is observed. Moreover, a prediction equation for the loading rate effect on the work of fracture is derived from the test data.

$$\begin{cases} W_F = W_F^S(1+m\dot{\delta}^r) = 147.5(1+0.34\dot{\delta}^{0.17}), & \text{for } \dot{\delta} < 7.04\times10^2 \text{ mm/s} \\ W_F = -26171.16 + 9296.4 log\dot{\delta}, & \text{for } \dot{\delta} \geq 7.04\times10^2 \text{ mm/s} \end{cases} \quad (4)$$

where W_F^S is the work of fracture and the static work of fracture. Exponents m and r are adjusting parameters, $\dot{\delta}$ is the loading rate given in mm/s. Eq. 4 can be used to efficiently predict the loading rate effect on work of fracture and could also be helpful when performing numerical simulations. It is worth to note that 147.5 *N/m* obtained by fitting is the static value of the work of fracture, and it could only be obtained by a strictly static test [25].

Under low loading rates, less than threshold, 7.04×10^{2} mm/s, the rate effect is mild, and it can be attributed to viscous effects mainly originated by the presence of free water in the voids and porous structures. Moreover, dry concrete exhibits very little rate sensitivity, except at very high strain rates also gives the reason of this tendency in another viewpoint [26].

However, under impact loading rates, greater than a threshold, the rate effect is remarkable due to the inertia effect [27-29]. Furthermore, the high increase in the work of fracture is caused by many micro-cracks that develop under impact loading [27,30,31]. Namely, at high loading rates the mechanism of failure is characterized by the propagation of many micro-cracks at the same time, and also

the micro-cracking does not have sufficient time to search for paths of minimum energy or lowest resistance. Thus, they are forced to propagate along the shortest path with higher resistances, this leads directly to the conclusion that the work of fracture should increase as a function of the loading rate.

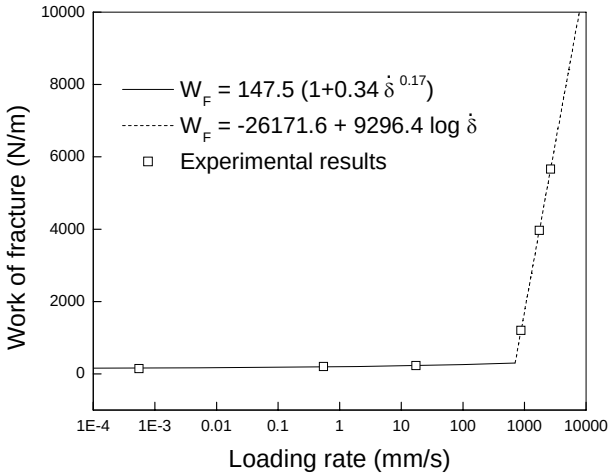

Fig. 2. Loading-rate dependence of the work of fracture

Fig. 3 shows the loading rate effect on the peak load, the tendency is similar with that of the work of fracture. Namely, under low loading rates, the tendency is moderate, while it is dramatic instead under high loading rates. The maximum DIF for the peak load is 7.14, compared with 38.12 for the work of fracture. Maybe the work of fracture is more sensitive to micro-cracks than the peak load under high loading rates. This also makes it possible to use only one exponential function to describe the behavior of peak load versus loading rates. Fig. 4 presents the function as well, namely,

$$P_{\max} = P_{\max}^{S}(1 + k\dot{\delta}^{n}) = 5.88(1 + 0.10\dot{\delta}^{0.51}) \tag{5}$$

where $P_{\max}^{S}$ is the static peak load, exponents *k* and *n* are adjusting parameters. It is noteworthy that the fitting also gives the static value of the peak load, 5.88 kN.

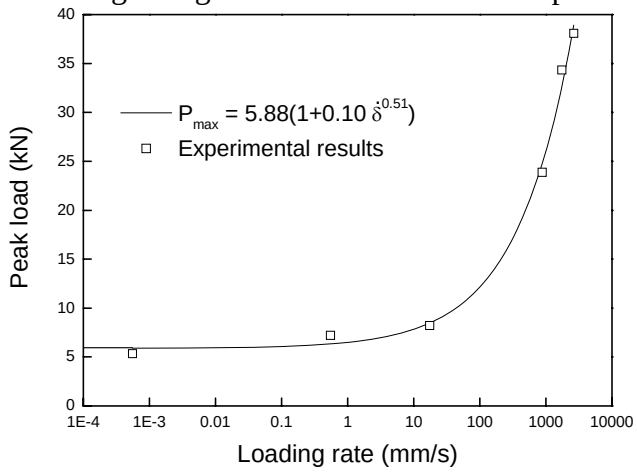

Fig. 3. Loading-rate dependence of the peak load

4. Comparison with data in the literature

As mentioned before, compared with the extensive research into the quasi-static fracture behaviour of HSC, much less information is available on its rate-sensitivity behaviour. Table 3 presents the comparison of some impact experimental results from S. Mindess [32] and to the results presented above.

From this table, it is clear that the trend of loading rate effect on mechanical properties of both high strength concretes is similar, though a little big difference on DIF for the peak load is found. In general, the weight of the hammer, the impact energy and the dimensions of the beams do affect the experimental results. Nevertheless, the results from different drop-weight impact machines are comparable.

Schuler [33] measured the tensile strength and the fracture energy (work of fracture) of High Performance Concrete (HPC) at high strain rates between 10 /s and 100 /s with spalling tests. A *DIF* of 3 at a crack opening velocity of 1.7 m/s on the fracture energy was observed. It is quite different in comparison to the experimental results with drop-weight impact tests, maybe this can partly be attributed to the inconsistency among the methods of loading and associated errors.

Furthermore, under low loading rates, the rate sensitivity of work of fracture is slight compared with the work of fracture variation at high loading rates. This leads some authors to conclude that the work of fracture is constant and rate independent at low loading rates [34-36].

Table 3 Comparison of experimental results

	Experimental results from S. Mindess et al. [32]	Experimental results in this paper
Compressive strength (MPa)	62	127
Dimension of the beam (width × depth × length) (mm)	100×125×1400	100×100×400
Span (mm)	960	300
Drop height of the hammer (mm)	150	160
Weight of the hammer (kg)	345	120.6
DIF for peak load	2.96	6.44
DIF for work of fracture	21.38	26.74

5. Conclusions

The fracture behaviour of a high strength concrete under dynamic loading conditions was investigated in this study. The loading rates varied widely from a

quasi-static level to a dynamic level, the order of magnitude changed from 10^{-4} mm/s to 10^{3} mm/s. As a result of the study, the following conclusions can be drawn.

(1) The work of fracture is sensitive to the loading rate. Under low loading rates, below 7.04×10^{2} mm/s, the rate effect is mild, and can be attributed to viscous effects mainly originated by the presence of free water in voids and porous structures. However, it is pronounced when the loading rate goes beyond the threshold. Finally, two prediction-equation of rate sensitivity for the work of fracture are proposed.

(2) The peak load shows similar tendency with the work of fracture to loading rates, while under high loading rates, the work of fracture is more sensitive to loading rates than the peak load. Moreover, also an exponential formula is provided.

(3) The formulas provided are helpful in numerical simulations that evaluate the rate dependence of fracture behavior.

Acknowledgements

Funding from the *Ministerio de Ciencia e Innovación*, Spain, under grant MAT2006-09105 and from the *Consejería de Educación y Ciencia*, JCCM, Spain, under grant PAI08-0196, is gratefully acknowledged.

References

[1] A. Yan, K.R. Wu, D. Zhang, W. Yao, Effect of fracture path on the fracture energy of high-strength concrete, Cement and Concrete Research, 31 (11) (2001) 1601-1606

[2] R.A. Einsfeld, M.S.L. Velasco, Fracture parameters for high-performance concrete, Cement and Concrete Research, 36 (3) (2006) 576-583

[3] J. Zhang, Q. Liu, L. Wang, Effect of coarse aggregate size on relationship between stress and crack opening in normal and high strength concretes, Journal of Materials Science and Technology, 21 (5) (2005) 691-700

[4] R.V. Sagar, S.V. Dinesh, A.C. Santosh, Fracture energy of normal and HSC beams, Indian Concrete Journal, 79 (11) (2005) 37-42

[5] B.H. Bharatkumar, B.K. Raghuprasad, D.S. Ramachandramurthy, R. Narayanan, S. Gopalakrishnan, Effect of fly ash and slag on the fracture characteristics of high performance concrete, Materials and Structures/Materiaux et Constructions, 38 (275) (2005) 63-72

[6] B. Chen, J. Liu, Effect of aggregate on the fracture behavior of high strength concrete, Construction and Building Materials, 18 (8) (2004) 585-590

[7] G. Appa Rao, B.K. Raghu Prasad, Strength and fracture toughness of interface in high strength concrete, Journal of Structural Engineering (Madras), 30 (3) (2003) 153-161
[8] F.H. Wittmann, Crack formation and fracture energy of normal and high strength concrete, Sadhana - Academy Proceedings in Engineering Sciences, 27 (4) (2002) 413-423
[9] G.A. Rao, B.K.R. Prasad, Fracture energy and softening behavior of high-strength concrete, Cement and Concrete Research, 32 (2) (2002) 247-252
[10] K.R. Wu, B. Chen, W. Yao, D. Zhang, Effect of coarse aggregate type on mechanical properties of high-performance concrete, Cement and Concrete Research, 31 (10) (2001) 1421-1425
[11] Z. Dong, W. Keru, Fracture properties of high-strength concrete, Journal of Materials in Civil Engineering, 13 (1) (2001) 86-88
[12] D. Darwin, S. Barham, R. Kozul, S. Luan, Fracture energy of high-strength concrete, ACI Materials Journal, 98 (5) (2001) 410-417
[13] Q. Li, F. Ansari, High-strength concrete in uniaxial tension, ACI Structural Journal, 97 (1) (2000) 49-57
[14] R. Gettu, V.O. Garcia-Álvarez, A. Aguado, Effect of aging on the fracture characteristics and brittleness of a high-strength concrete, Cement and Concrete Research, 28 (3) (1998) 349-355
[15] H. Marzouk, Z.W. Chen, Fracture energy and tension properties of high-strength concrete, Journal of Materials in Civil Engineering, 7 (2) (1995) 108-116
[16] R. Gettu, Z.P. Bazant, M.E. Karr, Fracture properties and brittleness of high-strength concrete, ACI Materials Journal, 87 (6) (1990) 608-618
[17] G.V. Guinea, J. Planas, M. Elices, Measurement of the Fracture Energy Using 3-Point Bend Tests .1. Influence of Experimental Procedures, Materials and Structures, 25 (148) (1992) 212-218
[18] J. Planas, M. Elices, G.V. Guinea, Measurement of the Fracture Energy Using 3-Point Bend Tests .2. Influence of Bulk Energy-Dissipation, Materials and Structures, 25 (149) (1992) 305-312
[19] M. Elices, G.V. Guinea, J. Planas, Measurement of the Fracture Energy Using 3-Point Bend Tests .3. Influence of Cutting the P-Delta Tail, Materials and Structures, 25 (150) (1992) 327-334
[20] M. Elices, G.V. Guinea, J. Planas, On the measurement of concrete fracture energy using three-point bend tests, Materials and Structures, 30 (200) (1997) 375-376
[21] X.X. Zhang, G. Ruiz, R.C. Yu, A new drop-weight impact machine for studying fracture processes in structural concrete, Strain, (2008)
[22] P. Sukontasukkul, P. Nimityongskul, S. Mindess, Effect of loading rate on damage of concrete, Cement and Concrete Research, 34 (11) (2004) 2127-2134
[23] N. Banthia, S. Mindess, A. Bentur, M. Pigeon, Impact testing of concrete using a drop-weight impact machine, Experimental Mechanics, 29 (1) (1989) 63-69

[24] J. Planas, G.V. Guinea, M. Elices, Stiffness associated with quasi-concentrated loads, Materiaux et constructions, 27 (170) (1994) 311-318
[25] G. Ruiz, X.X. Zhang, J.R. Del Viso, R.C. Yu, J.R. Carmona, Influence of the loading rate on the measurement of the fracture energy of a high strength concrete, 25th Encuentro del Grupo Español de Fractura, Vol. 25, Sigüenza, Spain, 2008, pp. 793-798
[26] S. Mindess, J.F. Young, D. Darwin, Concrete, Prentice Hall, Pearson Education, Inc. United States of America, United States of America, 2003
[27] A. Brara, J.R. Klepaczko, Fracture energy of concrete at high loading rates in tension, International Journal of Impact Engineering, 34 (3) (2007) 424-435
[28] J. Weerheijm, J.C.A.M. Van Doormaal, Tensile failure of concrete at high loading rates: New test data on strength and fracture energy from instrumented spalling tests, International Journal of Impact Engineering, 34 (3) (2007) 609-626
[29] P. Rossi, F. Toutlemonde, Effect of loading rate on the tensile behaviour of concrete : Description of the physical mechanisms, Materials and Structures/Materiaux et Constructions, 29 (186) (1996) 116-118
[30] P.H. Bischoff, S.H. Perry, Compressive behaviour of concrete at high strain rates, Materiaux et constructions, 24 (144) (1991) 425-450
[31] I. Vegt, V.K. Breugel, J. Weerheijm, Failure mechanisms of conrete under impact loading, in: A. Carpinteri, P. Gambarova, G. Ferro, G. Plizzari (Eds.), Fracture Mechanics of Concrete and Concrete Structures, Taylor & Francis Group, Italy, Catania, 2007, pp. 579-587
[32] S. Mindess, N. Banthia, C. Yan, Fracture toughness of concrete under impact loading, Cement and Concrete Research, 17 (2) (1987) 231-241
[33] H. Schuler, H. Hansson, Fracture behaviour of High Performance Concrete (HPC) investigated with a Hopkinson-Bar, Journal De Physique. IV : JP, Vol. 134, Dijon, 2006, pp. 1145-1151
[34] D. Birkimer, R. Lindemann, Dynamic tensile test of concrete materials, ACI Materials Journal, 68 (8) (1971) 47-49
[35] J. Weerheijm, Concrete under impact tensile loading and lateral compression, PhD Thesis, Delft University of Technology, 1992
[36] H. Schuler, C. Mayrhofer, K. Thoma, Spall experiments for the measurement of the tensile strength and fracture energy of concrete at high strain rates, International Journal of Impact Engineering, 32 (10) (2006) 1635-1650